Chapter 13

HOT DEFORMATION AND DYNAMIC RESTORATION

13.1 INTRODUCTION

The softening (restoration) processes of recovery and recrystallization may occur **during** deformation at high temperatures. In this case the phenomena are called **dynamic recovery** and **dynamic recrystallization** in order to distinguish them from the **static annealing** processes which occur during post-deformation heat treatment and which have been discussed in earlier chapters. The static and dynamic processes have many features in common, although the simultaneous operation of deformation and softening mechanisms leads to some important differences. Although dynamic restoration processes are of great industrial significance, they are not well understood because they are difficult to study experimentally and to model theoretically.

Dynamic recovery and dynamic recrystallization form part of the much larger subject of **hot working.** This is a very large and important area which cannot be covered in detail here. Some aspects of the historical development of the understanding of dynamic restoration are discussed by McQueen (1981) and Tegart (1992).

Dynamic recovery and dynamic recrystallization occur during metalworking operations such as **hot rolling, extrusion** and **forging.** They are important because they lower the flow stress of the material, thus enabling it to be deformed more easily and they also have an

influence on the texture and the grain size of the worked material. Dynamic recrystallization may also occur during creep deformation (Gifkins 1952, Poirier 1985), the main difference between **hot working** and **creep** being the strain rate. Hot working is generally carried out at strain rates in the range of 1–100 s^{-1}, whereas typical creep rates are below 10^{-5} s^{-1}. Nevertheless, in many cases similar atomistic mechanisms occur during both types of deformation. Dynamic recrystallization also occurs during the natural deformation of minerals in the Earth's crust and mantle, and is therefore of interest to Structural Geologists (e.g. Nicolas and Poirier 1976, Poirier 1985).

13.2 DYNAMIC RECOVERY

In metals of high stacking fault energy, such as aluminium and its alloys, α-iron and ferritic steels, dislocation climb and cross-slip occur readily (§2.2.2). Dynamic recovery is therefore rapid and extensive at high temperatures and is usually the only form of dynamic restoration which occurs. The stress-strain curve in this case is typically characterised by a rise to a plateau followed by a constant or steady state flow stress as shown in figure 13.1.

During the initial stages of deformation there is an increase in the flow stress as dislocations interact and multiply. However, as the dislocation density rises, so the driving force and hence the rate of recovery increases (§6.3), and during this period a microstructure of low angle boundaries and subgrains develops. At a certain strain, the rates of work hardening and recovery reach a dynamic equilibrium, the dislocation density remains constant and a **steady-state flow stress** is obtained as seen in figure 13.1. During deformation at strain rates larger than $\sim$1 s^{-1} the heat generated by the work of deformation cannot all be removed from the specimen and the temperature of the specimen rises during deformation. This may then cause a reduction in the flow stress as

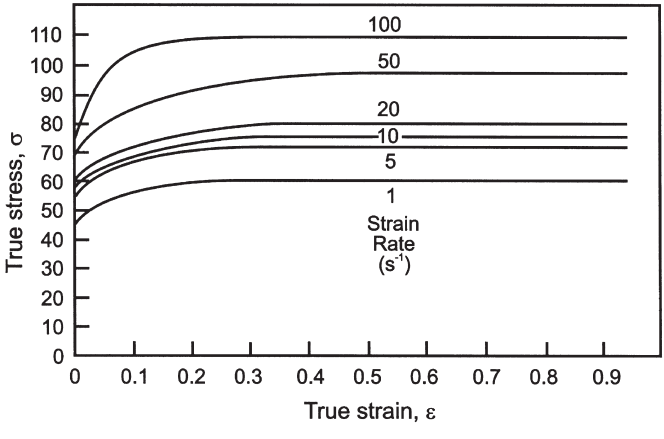

Fig. 13.1. Stress-strain curves for Al–1%Mg at 400°C, (Puchi et al. 1988).

straining proceeds. In modelling the high temperature deformation behaviour as discussed below, it is very important that such effects are taken into account (e.g. Shi et al. 1997).

13.2.1 Constitutive relationships

At temperatures where thermally activated deformation and restoration processes occur, the microstructural evolution will be dependent on the **deformation temperature (T)** and **strain rate** ($\dot{\varepsilon}$) in addition to the **strain** (ε). The strain rate and deformation temperature are often incorporated into a single parameter – **The Zener–Hollomon parameter (Z),** which is defined as:

$$Z = \dot{\varepsilon} \exp\left(\frac{Q}{RT}\right) \tag{13.1}$$

where Q is an activation energy.

For the purposes of analytical or computer modelling of hot working operations it is necessary to express the relationship between flow stress, temperature, strain and strain rate algebraically. If the flow stress follows a mechanical equation of state, i.e. it is dependent only on the **instantaneous** values of **T,** ε and $\dot{\varepsilon}$ and not on their **history,** then the relationship between these parameters may be expressed by relatively simple empirical equations (e.g. Jonas et al. 1969, Frost and Ashby 1982). It is found that during hot work, such a mechanical equation of state is closely followed, and during steady state deformation, the relationship between the flow stress (σ) and Zener–Hollomon parameter is often found to be

$$Z = c_1 \sinh(c_2\sigma)^n \tag{13.2}$$

where c_1, c_2 and n are constants.

Equation 13.2 may also be expressed in the form

$$\sigma = \frac{1}{c_2}\ln\left[\left(\frac{Z}{c_1}\right)^{1/n} + \left(\left(\frac{Z}{c_1}\right)^{2/n} + 1\right)^{1/2}\right] \tag{13.3}$$

At low values of stress, equation 13.3 reduces to a power relationship of the form

$$\dot{\varepsilon} = c_3\sigma^m \exp\left(-\frac{Q_1}{RT}\right) \tag{13.4}$$

where c_3, m and Q_1 are constants.

and at high stress values it simplifies to

$$Z = 0.5^n\ c_1 \exp(nc_2\sigma) = c_4 \exp(c_5\ \sigma) \tag{13.5}$$

Thus **Z** is seen to be closely related to the flow stress and hence to the dislocation density (equation 2.2). The Zener–Hollomon parameter is particular convenient for discussions of hot working processes in which the temperature and strain rate are generally known, whereas the flow stress may not be measurable.

A detailed consideration of the mechanical properties during hot deformation, the constitutive relationships and the microstructures developed during high temperature deformation is outside the scope of this book and further details may be found in Jonas et al. (1969), Roberts (1984, 1985), Sellars (1978, 1986, 1990, 1992a, 1992b), Blum (1993), Shi et al. (1997) and Davenport et al. (2000).

13.2.2 Mechanisms of microstructural evolution

The basic mechanisms of dynamic recovery are dislocation climb, cross-slip and glide, which result in the formation of low angle boundaries as also occurs during static recovery (§6.4). However, the applied stress provides an additional driving pressure for the movement of low angle boundaries and those of opposite sign will be driven in opposite directions, and this stress-assisted migration of dislocation boundaries may contribute significantly to the overall strain (Exell and Warrington 1972, Biburger and Blum 1992, Huang and Humphreys 2002). Such migration results in some annihilation of dislocations in opposing boundaries and Y-junction boundary interactions (§6.5.3) and these enable the subgrains to remain approximately equiaxed during the deformation. In-situ SEM deformation experiments have shown that some reorientation of subgrains may also occur during hot deformation. The subgrains can therefore be considered to be **transient** microstructural features.

The processes of work hardening and recovery lead to the continual formation and dissolution of low angle boundaries and to a constant density of unbound or 'free' dislocations within the subgrains. After a strain of typically 0.5 to 1, the subgrain structure often appears to achieve a steady state. The microstructural changes occurring during dynamic recovery are summarised schematically in figure 13.2, and typical microstructures are shown in figure 13.3.

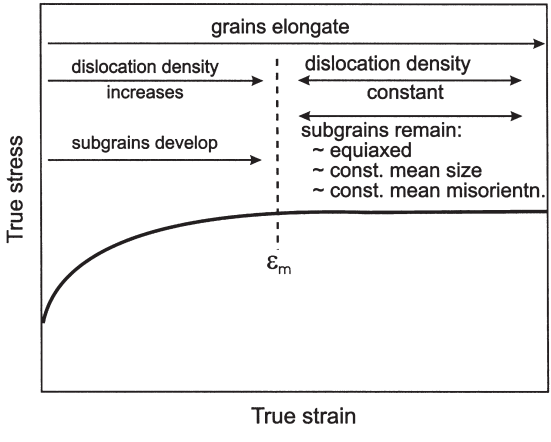

Fig. 13.2. Summary of the microstructural changes which occur during dynamic recovery, (after Sellars 1986).

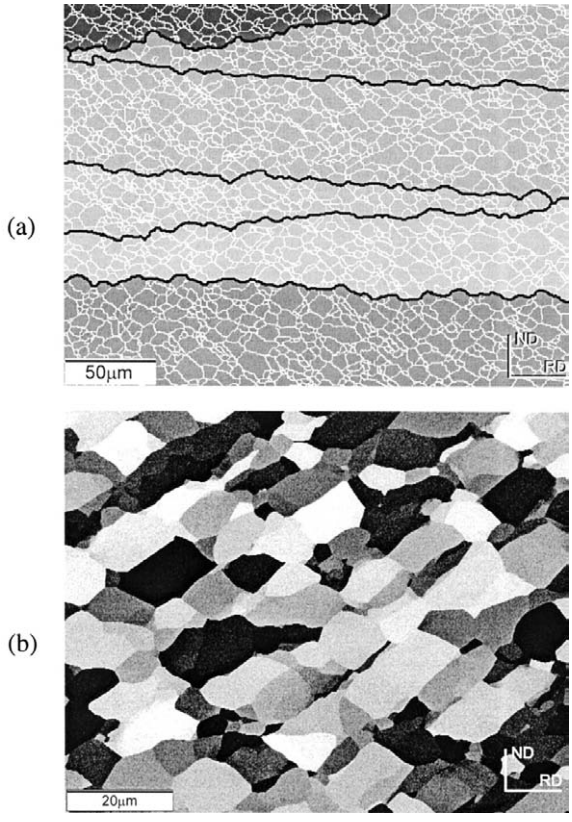

Fig. 13.3. Microstructure in ND-RD plane of Al–0.1%Mg deformed in plane strain compression at 350°C, $\varepsilon = 1$, $\dot{\varepsilon} = 0.25$. (a) EBSD map showing LAGBs (white) and serrated HAGBs (black), (b) SEM channelling contrast image showing the subgrain structure.

Although the dislocation and subgrain structures often remain approximately constant during steady-state deformation, the original grain boundaries do not migrate significantly and the grains continue to change shape during the deformation. This of course means that although the flow stress may remain constant, **a true microstructural steady state is not achieved** during dynamic recovery. This is particularly true if the strain is sufficient to reduce the separation of high angle boundaries to a value comparable with the subgrain size, an important situation which is further considered in chapter 14.

13.2.3 The microstructures formed during dynamic recovery

13.2.3.1 The subgrains

During high temperature deformation, dynamic recovery results in more organised dislocation arrangements within the subgrain boundaries (McQueen 1977), in the same

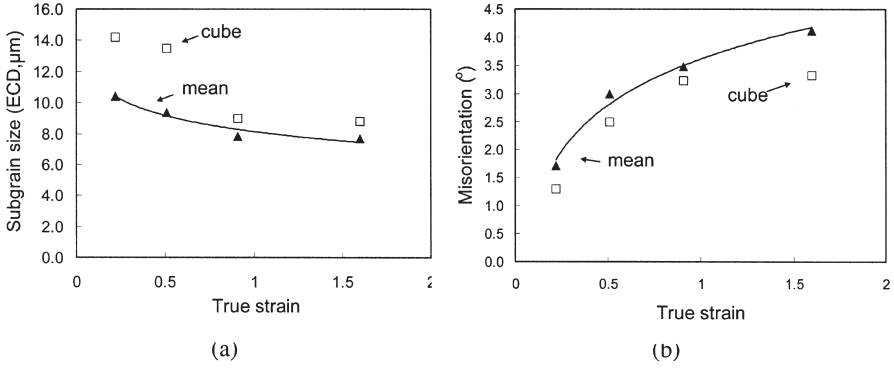

Fig. 13.4. The effect of strain on the size and misorientation of subgrains in Al–0.1Mg deformed in plane strain compression at 350°C at a rate of 10^{-2} s^{-1}. Both mean data, and data for cube-oriented subgrains are shown (Humphreys and Ashton 2003).

way as in static recovery (§6.4 and figure 6.13). In aluminium alloys, the cells or subgrains formed during low temperature deformation are arranged in bands, which are usually aligned on planes of high shear stress (see §2.4.2). This type of alignment is also found after high temperature deformation (Duly et al. 1996, Zhu and Sellars 2001), although it becomes less obvious at higher temperatures or lower strain rates (i.e. lower **Z**) as may be seen from a comparison of figures 2.10 and 13.3b.

The cell or subgrain size is generally found to be independent of strain at strains larger than ~0.5 (e.g. Duly et al. 1996), and as shown in figure 13.4a, although it depends on the temperature and rate of deformation (§13.2.3.4). However, the subgrain misorientations increase with strain as shown in figure 13.4b.

The subgrains formed during high temperature deformation are usually found to contain significant numbers of dislocations which are not associated with the low angle grain boundaries, and the density of these unbound dislocations has been found to be related to the flow stress (§13.2.3.4).

13.2.3.2 High angle boundary serrations

During deformation under conditions of low **Z,** the grain boundaries migrate locally in response to the boundary tensions of the substructure and to local dislocation density variations, and become serrated with a wavelength which is closely related to the subgrain size as shown in figures 13.3a and 13.5a. However, if small second-phase particles are present, these may prevent local migration of the high angle boundaries, so that these remain planar as shown in figure 13.5b.

13.2.3.3 The homogeneity of deformation

As discussed in chapter 2, the microstructures developed during low temperature deformation are usually very inhomogeneous and these regions of inhomogeneity are

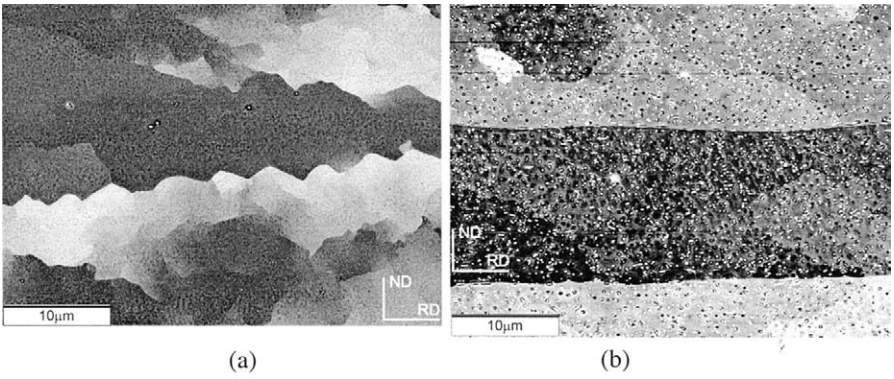

Fig. 13.5. High angle grain boundaries in aluminium alloys deformed at 400°C in plane strain compression. (a) Al–5%Mg, showing serrations at the high angle boundaries, (b) Al–2%Cu. Second-phase particles prevent boundary serrations from developing.

frequently sites for the origin of recrystallization during subsequent annealing. It is generally found that as the temperature of deformation increases, the deformation becomes more homogeneous (e.g. Drury and Humphreys 1986, Hansen and Jensen 1991, Ball and Humphreys 1996). Some of this may be explained in terms of an increase in the number of operating slip systems, which gives rise to homogeneous deformation more typical of the ideal 'Taylor type' plasticity (§3.7.1.2) than that which occurs at lower temperature. During deformation at high temperatures, slip systems which do not operate at low temperatures because of a higher Peierls–Nabarro stress may also become active. This is particularly important in non-metals and non-cubic materials, (Hazif et al. 1973, Ion et al. 1982) and even in face-centred cubic metals there is some evidence that slip systems other than $\{111\}<011>$ may operate at high temperatures (§13.2.4). Figure 13.6 shows how the frequency of the formation of the large-scale **deformation bands** visible under the optical microscope, decreases as the deformation temperature increases. Samajdar et al. (2001) have also shown that the long range misorientation gradients in aluminium, decrease as **Z** decreases. It is also usually found that **shear banding** becomes less frequent at higher deformation temperatures, as shown in figure 2.23.

13.2.3.4 The effect of the deformation conditions

The mechanisms of dislocation generation and recovery discussed above, operate over a wide range of temperatures and strain rates (e.g. Blum 1993). However, it should be noted that at very low strain rates and high temperatures (i.e. creep conditions), other mechanisms such as Herring–Nabarro and Coble creep may be important, although they will not be considered here. At low temperatures and high strain rates (high **Z**) the dislocation generation (work hardening) factor is dominant whereas at high temperatures and low strain rates (low **Z**) dynamic recovery dominates. Therefore after hot deformation, the microstructure will be dependent on both strain and Zener–Hollomon parameter.

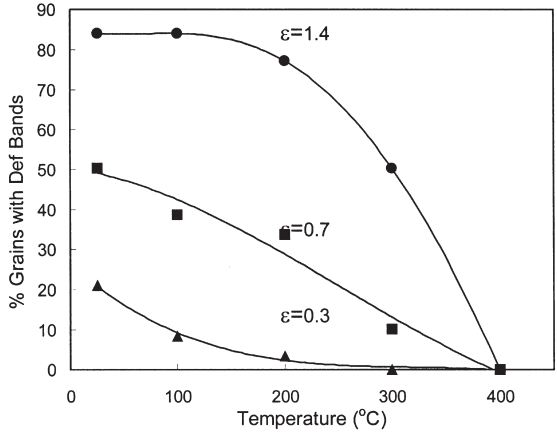

Fig. 13.6. The effect of deformation temperature and strain on the formation of large-scale deformation bands in Al–0.3Mn deformed in plane strain compression (Ball and Humphreys 1996).

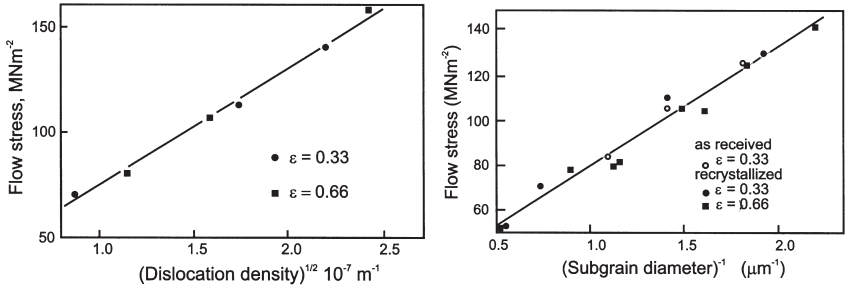

(a) (b)

Fig. 13.7. The relationship between the high temperature flow stress and microstructure in Al–1%Mg–1%Mn. (a) The dislocation density within subgrains (Castro–Fernandez et al. 1990), (b) The subgrain size, (Castro–Fernandez and Sellars 1988).

- **Dislocation content**

It has been found for steels and for aluminium that the high temperature flow stress is related to the density of dislocations **within** the subgrains (ρ_i) by the relationship (Castro–Fernandez et al. 1990)

$$\sigma = c_1 + c_2 G b \rho_i^{1/2} \tag{13.6}$$

where c_1 and c_2 are constants.

This is similar to the relationship between the flow stress and overall dislocation density found at low temperatures (equation 2.2), and figure 13.7a shows this relationship for an Al–Mg–Mn alloy.

- **Subgrain size**

If subgrains are formed, it is usually found (Sherby and Burke 1967) that the high temperature flow stress is inversely proportional to the mean subgrain diameter (**D**) (equation 6.30) and an example of this is shown in figure 13.7b. It has been shown (Takeuchi and Argon 1976) that if equation 6.30 is expressed in terms of normalised stress and subgrain size and a dimensionless constant K, then K is constant for any particular class of material.

$$\frac{\sigma}{G}\frac{D}{b} = K \tag{13.7}$$

Derby (1991) has analysed subgrain data for a range of metals and minerals and these are plotted according to equation 13.7 in figure 13.8. **K** has a value of ~10 for fcc metals and ~25–80 for ionic crystals of the NaCl structure.

Furu et al. (1992) have analysed subgrain sizes in aluminium alloys for a wide range of conditions, and shown that the relationship between subgrain size (D) and Zener–Hollomon parameter (**Z**) for $10^{13} < Z < 10^{17}$ can be expressed empirically as

$$D = K_1 - K_2 \log Z \tag{13.8}$$

where k_1 and k_2 are constants.

At constant flow stress (or **Z**), equations 13.6 and 6.30 imply a unique relationship between the subgrain size and the dislocation density within the subgrains of the form

$$\rho_i^{1/2} = c_3 D^{-1} \tag{13.9}$$

Such a relationship is predicted by theoretical models of subgrain formation during deformation (e.g. Holt 1970, Edward et al. 1988), and experimental investigations in

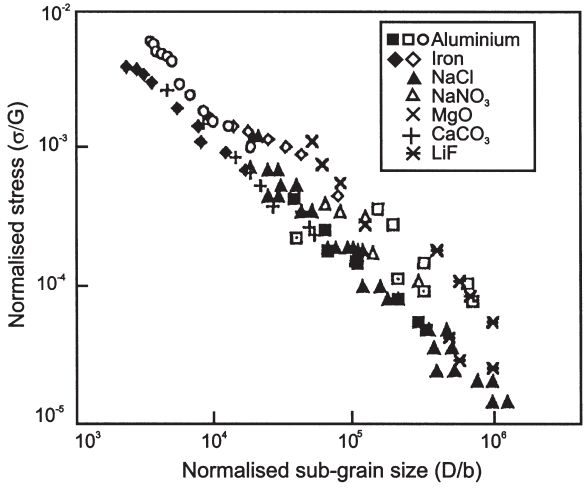

Fig. 13.8. The relationship between subgrain size and high temperature flow stress, (after Derby 1991).

aluminium (Castro–Fernandez et al. 1990), copper (Straker and Holt 1972) and ferritic steels (Barrett et al. 1966, Urcola and Sellars 1987), have reported values of c_3 between 10 and 20.

13.2.3.5 The effect of variable deformation conditions

During many hot working operations, the deformation temperature and strain rate do not remain constant, and because the microstructural parameters such as dislocation density are closely linked to the deformation conditions as discussed in the previous section, an understanding of microstructural evolution under conditions of varying temperature or strain rate is important. Hot deformation experiments on aluminium alloys, in which the strain rate is raised during deformation (Baxter et al. 1999), have shown that the microstructures reach equilibrium after little further deformation. However, if the strain rate is decreased during deformation, further strains of ~0.5 are required before the microstructure achieves steady state values. Huang and Humphreys (2002) found that the main mechanism of subgrain growth during a strain rate decrease was by low angle boundary migration. The rate of subgrain growth under these conditions is very much larger than for static annealing as shown in figure 13.9, the boundary migration rates being strongly affected by the imposed stress (§13.2.2).

13.2.4 Texture formation during hot deformation

The crystallographic textures resulting from cold or warm deformation were discussed in chapter 3. In some cases deformation at high temperatures may produce significantly

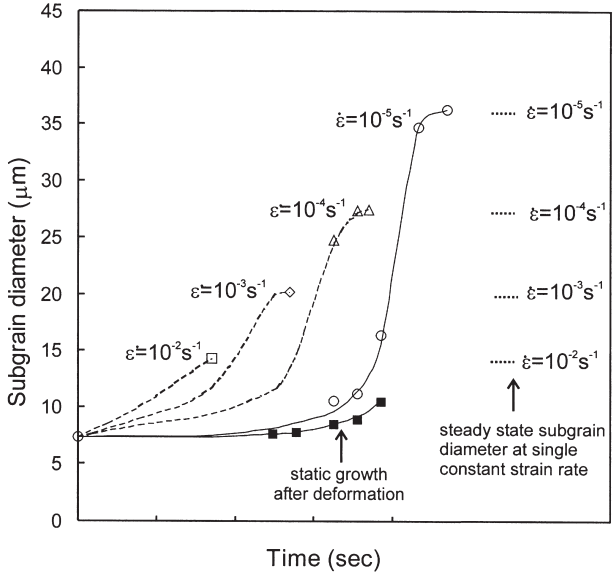

Fig. 13.9. The effect of strain rate change on samples of commercially pure aluminium, initially deformed to a strain of 0.9 at 400°C a rate of 0.5 s^{-1}. The growth rates of the subgrains under static conditions are also shown (Huang and Humphreys 1997).

different textures, even in materials which undergo only dynamic recovery. Because these textures may have a strong influence on the recrystallization of hot-worked material, we will give a brief discussion here, and focus particularly on the cube texture component in hot-deformed aluminium alloys. This topic is of great industrial significance, and has been the subject of extensive research in recent years.

As discussed in §13.2.1, the deformation temperature and strain rate are conveniently described collectively by the Zener–Hollomon parameter (**Z**). The textures developed in aluminium alloys during deformation under conditions of low **Z,** often differ from those in alloys deformed at ambient temperatures (high **Z**), and in particular, it is found that during plane strain compression (e.g. rolling), there is increasing stability of the $\{011\}<211>$, Brass, and $\{001\}<100>$, Cube, components at the expense of the other normal rolling components as **Z** decreases.

The texture of a commercially hot-rolled Al–1%Mn–1%Mn alloy is shown in figure 13.10. It may be seen that the normal rolling texture components, Brass, Copper and S (see fig. 3.3) are all present, but that along the β-fibre, the Brass component is particularly strong, and that there are also peaks close to Cube.

Some care has to be taken in interpreting hot deformation textures as true deformation textures, because of the possibility of some recrystallization occurring prior to quenching, and this is particularly true for Al–Mg alloys (e.g. Hirsch 1991). Details

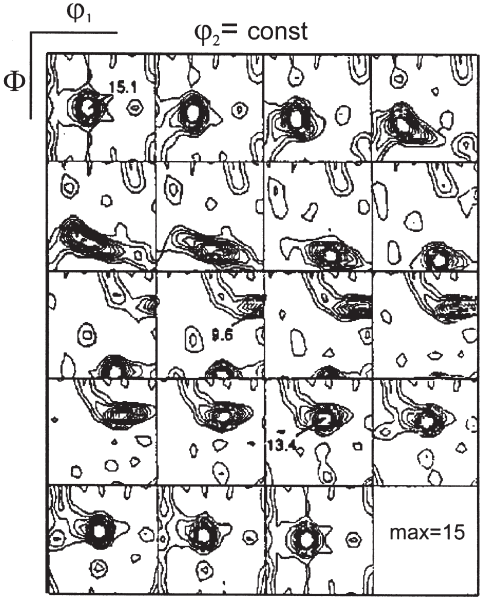

Fig. 13.10. ODF of commercially hot-rolled Al–1%Mg–1%Mn alloy showing a large Brass component and a significant Cube component in addition to the normal rolling texture, (Daaland and Nes 1995).

of the texture evolution also depend strongly on the starting texture (Bolingbroke et al. 1995), but the above trends are generally observed, and are consistent with studies of hot-deformed single crystals (Maurice and Driver 1993, 1997a).

An investigation of textures after hot deformation in a number of dilute aluminium alloys (Vernon–Parry et al. 1996) showed that under the range of conditions studied, the strength of the cube texture decreased with increasing strain, and decreased with increasing **Z.** Similar results were reported by Basson et al. 1998, and their results are shown in figure 13.11.

It is also found that the subgrains within different texture components have different characteristics. Table 13.1 shows TEM measurements for subgrains in an Al–1Mg alloy deformed in plane strain compression at 400°C to a strain of 1. The last column shows the stored energy, which is a function of the subgrain misorientation divided by the size (equation 2.8). These measurements, together with those of Bardal et al. (1995) on Al–1%–1%Mg, and the data of figure 13.4, indicate that while cube-oriented subgrains in aluminium tend to be larger than other subgrains, they have similar or somewhat lower misorientations. This is thought to be an important factor in the subsequent recrystallization of hot-deformed aluminium (§13.6.2) and the development of recrystallization texture (§12.4.1).

The increased stability of the Brass and Cube texture components in aluminium alloys during high temperature deformation has been explained by the operation of non-octahedral slip, $\{110\}<110>$, at high temperatures, for which there is some evidence from surface slip markings (Hazif et al. 1973, Maurice and Driver 1993). If such slip is included in crystal plasticity calculations, then an increased stability of these texture components can be predicted (Maurice and Driver 1993, 1997b). However, the agreement between predicted and actual textures is not particularly good if reasonable

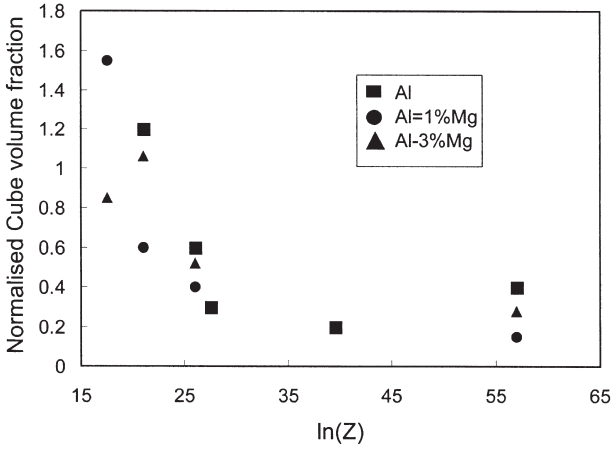

Fig. 13.11. Normalised cube texture volume fraction as a function of Zener–Hollomon parameter (Z), for alloys deformed in plane strain compression to a strain of 1, (after Basson et al. 1998).

Table 13.1
Subgrain parameters in an Al–1Mg alloy deformed at 400°C to $\varepsilon = 1$ (Driver et al. 1996).

Orientation	Misorientation (deg)	Size (μm)	Stored Energy ($mJcm^{-3}$)
Brass	3.1	12	12.2
S	6.3	17	13.3
Copper	4.3	14	12.9
Cube	4	23	7.6

slip conditions are assumed (Kocks et al. 1994, Knutsen et al. 1999, Samajdar et al. 2001). Additionally, the occurrence of non-octahedral slip cannot easily explain why the strength of the cube texture may, in certain circumstances actually increase with strain (Knutsen et al. 1999). Several authors have linked the changes in texture to changes in microstructure (Samajdar et al. 2001) and to the onset of some form of dynamic grain boundary migration (Kocks et al. 1994, Knutsen et al. 1999), and further work is required to clarify this matter.

13.2.5 Modelling the evolution of microstructure

There is a significant interest in modelling the evolution of microstructure during the hot deformation of metals which undergo dynamic recovery. The aims are to predict both the microstructures and the flow stresses of materials processed under the wide range of conditions employed in industrial processing, and a comprehensive review of the subject is given by Shercliff and Lovatt (1999). The early work was based on the development of the empirical constitutive equations discussed in §13.2.1, but more recently, most attention has been given to the development of 'physically based' state variable models in which models which quantify parameters such as dislocation density, subgrain size and misorientation are combined to model the overall microstructural evolution. Examples of this type of modelling may be found in the work of Sellars (1990, 1997), Nes (1995b), Nes and Furu (1995), and Shercliff and Lovatt (1999). Such modelling has been extended by using finite element methods to provide more realistic descriptions of the strain, strain rate and temperature distributions during deformation processing (McLaren and Sellars 1992, Beynon 1999, Davenport et al. 1999). Details of these models are outside the scope of this book, but an outline of how such models may be used in the context of industrial deformation processing is given in §16.3.3.

13.3 DISCONTINUOUS DYNAMIC RECRYSTALLIZATION

In metals in which recovery processes are slow, such as those with a low or medium stacking fault energy (copper, nickel and austenitic iron), dynamic recrystallization may take place when a critical deformation condition is reached. A simplified description of the phenomenon of dynamic recrystallization is as follows. New grains originate at the old grain boundaries, but, as the material continues to deform, the dislocation density of

the new grains increases, thus reducing the driving force for further growth, and the recrystallizing grains eventually cease to grow. An additional factor which may limit the growth of the new grains is the nucleation of further grains at the migrating boundaries.

This type of dynamic recrystallization, which has clear nucleation and growth stages, can be classified as a discontinuous process. There are other mechanisms which produce high angle grain boundaries during high temperature deformation, and which may be considered to be types of dynamic recrystallization. These phenomena are discussed in §13.4.

13.3.1 The characteristics of dynamic recrystallization

The general characteristics of dynamic recrystallization are as follows:

- As shown in figure 13.12, the stress-strain curve for a material which undergoes dynamic recrystallization generally exhibits a broad peak that is different to the plateau, characteristic of a material which undergoes only dynamic recovery (fig. 13.1). Under conditions of low Zener–Hollomon parameter, multiple peaks may be exhibited at low strains, as seen in figure 13.12.
- A critical deformation (ε_c) is necessary in order to initiate dynamic recrystallization. This occurs somewhat before the peak (σ_{max}) of the stress strain curve. For a range of testing conditions, σ_{max} is uniquely related to the Zener–Hollomon parameter (**Z**).
- ε_c decreases steadily with decreasing stress or Zener–Hollomon parameter, although at very low (creep) strain rates the critical strain may increase again (Sellars 1978).
- The size of dynamically recrystallized grains (D_R) increases monotonically with decreasing stress. Grain growth does not occur and the grain size remains constant during the deformation.

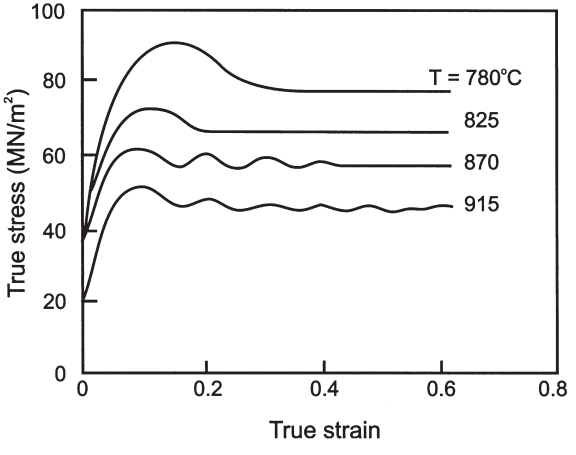

Fig. 13.12. The effect of temperature on the stress-strain curves for 0.68%C steel, deformed in axisymmetric compression, $\dot{\varepsilon} = 1.3 \times 10^{-3}\ s^{-1}$, (Petkovic et al. 1975).

- The flow stress (σ) and D_R are almost independent of the initial grain size (D_0), although the kinetics of dynamic recrystallization are accelerated in specimens with smaller initial grain sizes.
- Dynamic recrystallization is usually initiated at pre-existing grain boundaries although for very low strain rates and large initial grain sizes, intragranular nucleation becomes more important.

13.3.2 The nucleation of dynamic recrystallization

13.3.2.1 Nucleation mechanisms

Dynamic recrystallization originates at high angle boundaries. These may be the original grain boundaries, boundaries of dynamically recrystallized grains, or high angle boundaries created during straining (e.g. those associated with deformation bands or deformation twins). Bulging of grain boundaries is frequently observed as a prelude to dynamic recrystallization, and it is usually assumed that a mechanism closely related to strain-induced grain boundary migration (§7.6.2) operates. Recent investigations (Wusatowska et al. 2002), have suggested that the origin of dynamic recrystallization in copper may be the formation of lattice rotations at grain boundary serrations due to boundary sliding, a mechanism proposed by Drury and Humphreys (1986), which is discussed in §13.4.2.

13.3.2.2 Models of dynamic recrystallization

Several models of dynamic recrystallization have been proposed. Regardless of the details of the mechanism of nucleation, the condition for the growth of a dynamically recrystallized grain is thought to depend on the distribution and density of dislocations, both in the form of subgrains and free dislocations §13.2.3, which provide the driving force for growth. Figure 13.13, based on the model of Sandström and Lagneborg (1975), shows schematically the dislocation density expected in the vicinity of a migrating boundary. The boundary at **A** is moving from left to right into unrecrystallized material which has a high dislocation density ρ_m. As the boundary moves, it reduces the dislocation density in its wake to around zero by recrystallization. However, the continued deformation raises the dislocation density in the new grain, so that it builds

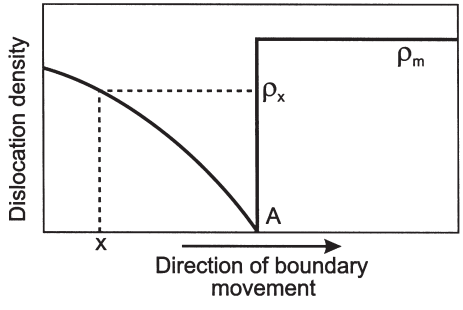

Fig. 13.13. Schematic diagram of the dislocation density at a dynamic recrystallization front, (after Sandström and Lagneborg 1975).

up behind the moving boundary and reaches ρ_x at a distance **x** behind the boundary, tending towards a value of ρ_m at large distances. The following very approximate analysis, which does not take dynamic recovery into account is based on that proposed by Sandström and Lagneborg (1975) and Roberts and Ahlblom (1978).

The migrating grain boundary moves under a driving pressure of $\sim\rho_m Gb^2$ arising from the dislocation density difference across the boundary and from equation 5.1, the resulting velocity is given as

$$\frac{dx}{dt} = M\rho_m Gb^2 \tag{13.10}$$

If the mean slip distance of the dislocations is **L,** the rate of increase of dislocation density behind the migrating boundary due to the continuing deformation is obtained by differentiating equation 2.1.

$$\frac{d\rho}{dt} = \frac{\dot{\varepsilon}}{bL} \tag{13.11}$$

and hence

$$\frac{d\rho}{dx} - \frac{\dot{\varepsilon}}{MLGb^3\rho_m} \tag{13.12}$$

and

$$\rho = \frac{\dot{\varepsilon}x}{MLGb^3\rho_m} \tag{13.13}$$

The dislocation density behind the moving boundary reaches the value of ρ_m when $x = x_c$ and hence

$$x_c = \frac{MLGb^3\rho_m^2}{\dot{\varepsilon}} \tag{13.14}$$

If nucleation is assumed to occur by a bulge mechanism, then the critical condition for the formation of a nucleus of diameter x_c would (equation 7.40) be

$$E > \frac{2\gamma_b}{x_c} \tag{13.15}$$

Where **E** is the stored energy, which is taken to be a fraction **K** of $\rho_m Gb^2$. Using equation 13.14, the condition for nucleation then becomes

$$\frac{\rho_m^3}{\dot{\varepsilon}} > \frac{2\gamma_b}{KMLGb^5} \tag{13.16}$$

The terms on the right hand side of equation 13.16 may be regarded as approximately constant at a particular temperature, and thus the condition for the nucleation of dynamic recrystallization is that a critical value of $\rho_m^3/\dot{\varepsilon}$ must be achieved. In materials such as aluminium and pure iron, recovery occurs readily and this parameter, strongly dependent on dislocation density, never reaches the critical value, and therefore only **dynamic recovery** occurs. However in materials of lower stacking fault energy such as

copper, nickel and stainless steel, recovery is slow and the dislocation density increases to the critical value necessary for **dynamic recrystallization** to occur.

There is some confusion in the literature about the occurrence of dynamic recrystallization in aluminium. As discussed above, rapid dynamic recovery generally prevents the accumulation of sufficient dislocations to sustain dynamic recrystallization. However, there have been numerous reports of dynamic recrystallization in aluminium of very high purity, and these have been reviewed by Kassner and Evangelista (1995), who conclude that discontinuous dynamic recrystallization can occur during room temperature deformation in very high purity aluminium. If we consider the conditions for dynamic recrystallization given by equation 13.16, we see that the critical value of $\rho_m^3/\dot{\varepsilon}$ required for dynamic recrystallization will be reduced by an increased boundary mobility (M), and as discussed in §5.3, very high boundary mobilities are found in very pure metals. Thus it is quite likely that there are conditions under which the increase in boundary mobility outweighs any increase in the recovery rate, thereby allowing dynamic recrystallization to occur.

13.3.3 Microstructural evolution

Dynamic recrystallization generally starts at the old grain boundaries as shown schematically in figure 13.14a. New grains are subsequently nucleated at the boundaries of the growing grains (fig. 13.14b), and in this way a thickening band of recrystallized grains is formed as shown in figure 13.14c. If there is a large difference between the initial grain size (D_0) and the recrystallized grain size (D_R), then a **'necklace'** structure of grains may be formed (fig. 13.14b–c), and eventually the material will become fully

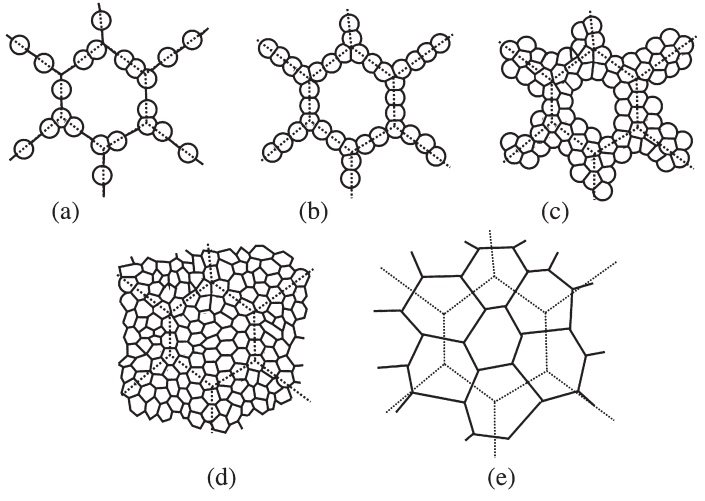

Fig. 13.14. The development of microstructure during dynamic recrystallization. (a)–(d) Large initial grain size, (e) small initial grain size. The dotted lines show the prior grain boundaries.

recrystallized (13.14d). A micrograph of copper which has undergone partial dynamic recrystallization is shown in figure 13.15.

Unlike static recrystallization, the mean size of the dynamically recrystallized grains does not change as recrystallization proceeds as shown in figure 13.16.

In some cases, microstructural evolution is more complicated than that described above, because the onset of dynamic recrystallization may lead to changes in deformation mechanism. For example, if dynamic recrystallization results in a very small grain size, then subsequent deformation may occur preferentially by the mechanism of **grain boundary sliding.** This will tend to occur if deformation by dislocation glide and climb is particularly difficult, and has been reported in α-brass (Hatherly et al. 1986) in which

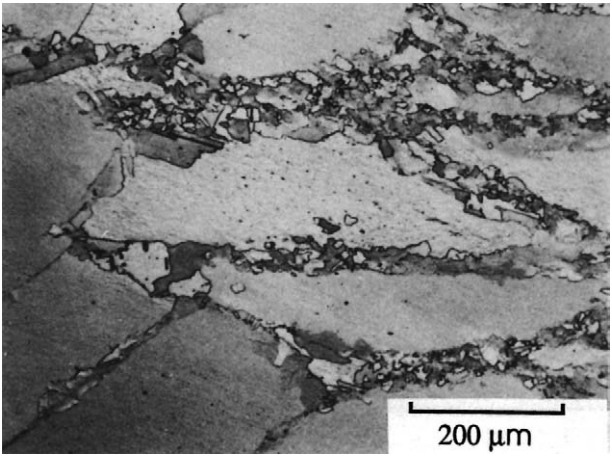

Fig. 13.15. Dynamic recrystallization at prior grain boundaries in polycrystalline copper at 400°C, $\dot{\varepsilon} = 2 \times 10^{-2}$, $\varepsilon = 0.7$, (Ardakani and Humphreys 1992).

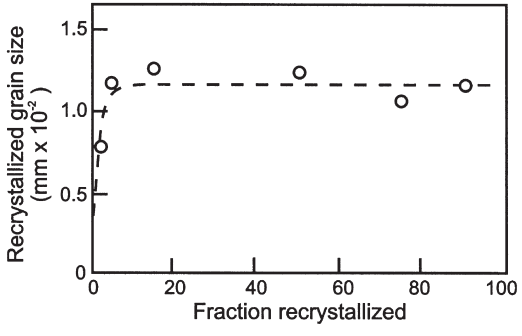

Fig. 13.16. Relationship between dynamically recrystallized grain size and fraction recrystallized in nickel deformed at 880°C, $\dot{\varepsilon} = 5.7 \times 10^{-2}$ s^{-1}, (Sah et al. 1974).

the low stacking fault energy hinders climb, in magnesium (Drury et al. 1989) where there are few slip systems, in dispersion hardened copper (Ardakani and Humphreys 1992) in which dislocation motion is hindered by second-phase particles, and in intermetallics (Ponge and Gottstein 1998).

13.3.4 The steady state grain size

Experimental observations generally show that the steady state grain size (D_R) during dynamic recrystallization is a strong function of the flow stress and is only weakly dependent on deformation temperature. The empirical relationship is often given as

$$\sigma = KD_R^{-m} \tag{13.17}$$

where $m < 1$ and K is a constant. Twiss (1977) examined the relation between the mean grain size and flow stress of a number of materials and proposed a universal relationship which can be expressed in normalised form as

$$\frac{\sigma}{G}\left(\frac{D_R}{b}\right)^n = K_1 \tag{13.18}$$

where $n = 0.8$ and $K_1 = 15$, which is of a rather similar form to the subgrain relationship of equation 13.7. Derby (1991) has found that such a relationship holds for a very wide range of materials of metallurgical and geological significance as shown in figure 13.17, and has shown that the data in figure 13.17 are bounded by loci of the form

$$1 < \frac{\sigma}{G}\left(\frac{D_R}{b}\right)^{2/3} < 10 \tag{13.19}$$

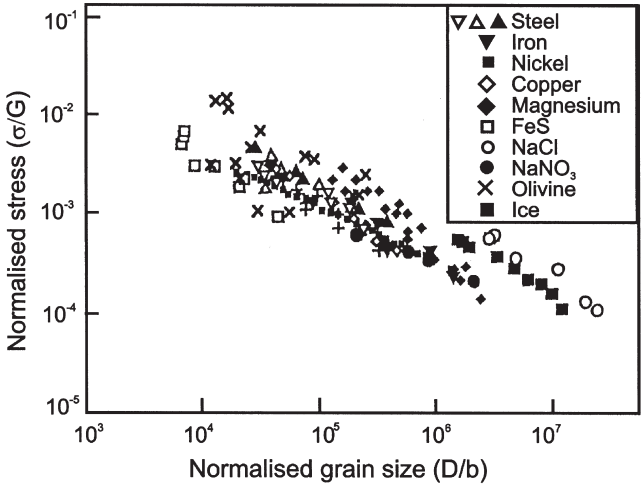

Fig. 13.17. The relationship between dynamically recrystallized grain size and high temperature flow stress, (after Derby 1991).

However, Wusatowska et al. (2002) have recently reported that in copper, although the grain size exponent (**m**) in equation 13.17 is 0.75 at low flow stresses, it reduces to 0.23 at high stress, suggesting a change in the mechanism of dynamic recrystallization.

Dynamic recrystallization is a continuous process of deformation, nucleation of grains and subsequent migration of grain boundaries, leaving new dislocation-free grains which then deform further. Although the details of dynamic recrystallization cannot be directly observed in metals, these processes have been observed to occur in transparent crystalline materials (§13.5).

For a steady state to occur there must be a dynamic balance between the nucleation of new grains and the migration of the boundaries of the previously nucleated grains. Derby and Ashby (1987) have analysed this balance as follows. In the time taken for a moving boundary to sweep out a volume equivalent to the mean steady state grain size (D_R), the nucleation rate ($\dot{N}$) should be sufficient for one new nucleation event to occur in each equivalent volume averaged over the microstructure. If nucleation is confined to pre-existing grain boundaries then this condition may be expressed as

$$\frac{CD_R^3\dot{N}}{\dot{G}} = 1 \tag{13.20}$$

where C is a geometric constant ~3.

The steady state grain size will therefore be dependent on the ratio of the nucleation and growth rates. Derby and Ashby (1987) argue that as the steady state grain size depends on the ratio of the nucleation and growth rates, both of which may have a similar temperature dependence, then it is to be expected that the steady state grain size will be only weakly dependent on temperature, as is found in practice. If the size of the dynamically recrystallized grains (D_R) is taken to be equal to x_c as given by equation 13.14, and we assume a relationship between flow stress and dislocation density of the form of equation 2.2 and a relationship between flow stress and strain rate as given by equation 13.4 with $m = 5$, then equation 13.14 may be written in the form $\boldsymbol{\sigma = K'/D,}$ which is similar to equation 13.18. Derby and Ashby (1987) have used a more sophisticated version of this analysis to calculate the steady state grain size starting from equation 13.20 and arrive at a relationship close to that of equation 13.18.

13.3.5 The flow stress during dynamic recrystallization

As shown in figure 13.12, the stress strain curves of a dynamically recrystallizing material may be characterised by a single peak or by several oscillations. Luton and Sellars (1969) have explained this in terms of the kinetics of dynamic recrystallization. At low stresses, the material recrystallizes completely before a second cycle of recrystallization begins, and this process is then repeated. The flow stress, which depends on the dislocation density, therefore oscillates with strain. At high stresses, subsequent cycles of recrystallization begin before the previous ones are finished, the material is therefore always in a partly recrystallized state after the first peak, and the stress strain curve is smoothed out, resulting in a single broad peak.

Sakai and Jonas (1984) have suggested that the shape of the stress strain curve depends primarily on the ratio of the recrystallized and starting grain sizes (D_0/D_R). If (D_0/D_R) > 2 then the microstructure develops as shown in 13.14a–d, the material is only partly recrystallized except at very high strains, and a smooth curve with a single peak results. However, if $D_0/D_R < 2$ then the new grains all develop at about the same time because there are enough sites (i.e. old boundaries) for recrystallization to be complete in one cycle as shown in figure 13.14e. This fully recrystallized and softened material then undergoes further deformation, hardens, and then recrystallizes again. As this cycle is repeated, an oscillatory stress strain curve results. The shape of the stress-strain curve therefore depends on the deformation conditions (Z) and on the initial grain size. Figure 13.18 illustrates schematically the relationship between the stress-strain behaviour and these parameters.

13.3.6 Dynamic recrystallization in single crystals

A considerable research effort has been expended in studying the fundamental aspects of the dynamic recrystallization of single crystals of silver, gold, nickel and copper and its alloys, and this is reviewed by Mecking and Gottstein (1978) and Gottstein and Kocks (1983). As discussed earlier in this chapter, dynamic recrystallization is essentially a grain boundary phenomenon, and therefore its occurrence in single crystals, although scientifically interesting, is unlikely to be of direct relevance to the thermomechanical processing of industrial alloys.

As shown in figure 13.19, the stress-strain curve of a copper crystal deformed in tension at high temperatures exhibits a sharp drop, which has been shown to correspond to the occurrence of dynamic recrystallization. There is no clear correlation between the strain and the onset of dynamic recrystallization, but the shear stress for dynamic recrystallization (τ_R) has been shown to be reproducible for given deformation conditions. However, τ_R is a function of the material, the crystal orientation, the

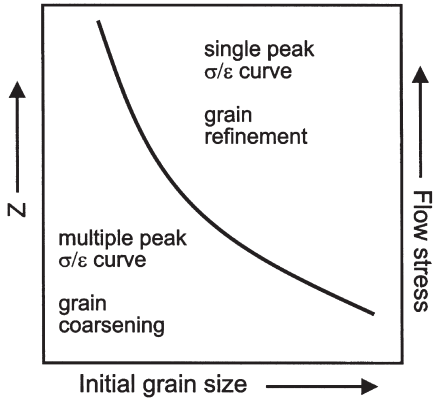

Fig. 13.18. The conditions for multiple and single peak dynamic recrystallization, (after Sakai et al. 1983).

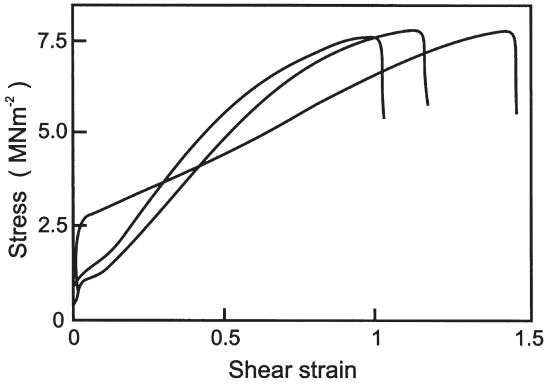

Fig. 13.19. Shear-stress/shear-strain curves of copper crystals of similar orientation deformed at 857°C, (Gottstein et al. 1979).

deformation temperature and the strain rate (Gottstein et al. 1979, Stuitje and Gottstein 1980, Gottstein and Kocks 1983), and unlike the case for polycrystals, τ_R is not uniquely related to the Zener–Hollomon parameter.

The experimental evidence suggests that in the high temperature regime, dynamic recrystallization in a single crystal is triggered by the formation of a single critical nucleus which is a subgrain in the deformed structure. This subgrain then sweeps rapidly through the microstructure. However in the low temperature regime, copious twinning of the nucleus takes place, and rapid growth only occurs when a twin with a high mobility orientation relationship with the matrix (§5.3.2) is formed. The onset of dynamic recrystallization in single crystals is therefore seen to be **nucleation controlled** in contrast to polycrystals (§13.3.4) in which it is **growth controlled.**

In single crystals of copper containing a fine dispersion of oxide particles which inhibit subgrain growth, dynamic recrystallization has been found to nucleate at the transition bands which form in the crystals during high temperature deformation (Ardakani and Humphreys 1992).

13.3.7 Dynamic recrystallization in two-phase alloys

There is some evidence that a process similar to the particle stimulated nucleation of recrystallization (PSN) which occurs on static annealing of alloys containing large particles (§9.3), may occur during high temperature deformation. In copper, dynamically recrystallized grains have been found at particles of SiO_2 or GeO_2 several microns in diameter (Ardakani and Humphreys 1992). The microstructures developed in these alloys are very different to those in single-phase copper (fig. 13.15), or in copper containing small particles, in which dynamic recrystallization is associated only with the prior grain boundary regions.

There is little evidence for particle stimulated dynamic recrystallization in aluminium alloys. Humphreys and Kalu (1987) and Castro–Fernandez and Sellars (1988) found

small highly misoriented grains adjacent to large second-phase particles, but these grains were generally of a similar size to the subgrains remote from the particles and there was little evidence of their growth. It is likely that such nuclei form by dynamic recovery of the misoriented subgrains formed at particles during deformation (§2.9.4), but that the stored energy of the matrix is too low to allow the nuclei to grow (§9.3). Although dynamic recrystallization in Al–Mg alloys has been attributed to PSN (McQueen et al. 1984, Sheppard et al. 1983), it is more likely that the recrystallized grains found in these alloys were formed by progressive lattice rotation as discussed in §13.4.2.

Particle stimulated dynamic recrystallization will only be possible if dislocations accumulate at the particles during deformation. This will only occur for larger particles, lower temperatures and higher strain rates (high **Z**) and therefore, unlike single phase alloys, there will be a particle-dependent lower limit to **Z** below which the nucleation of PSN will not be possible (fig. 13.31). This aspect is considered in more detail in §13.6.4.

13.3.7.1 Phase transformations during hot deformation

In addition to the processes of recovery and recrystallization, there may be concurrent phase transformations during deformation at elevated temperatures. The complex interactions between the processes of deformation, restoration and phase transformation are of great importance in the thermomechanical processing of a number of materials, in particular steels (Gladman 1990, Jonas 1990, Fuentes and Sevillano 1992) and titanium alloys (Williams and Starke 1982, Flower 1990, Weiss et al. 1990). Although we have discussed the underlying principles of many of the individual restoration processes involved, a detailed treatment of this subject is beyond the scope of this book.

13.4 CONTINUOUS DYNAMIC RECRYSTALLIZATION

13.4.1 Types of continuous dynamic recrystallization

The dynamic recrystallization discussed in §13.3 is the normal discontinuous dynamic recrystallization which occurs for example in cubic metals of low stacking fault energy. However, in recent years it has become apparent that under certain conditions a microstructure of high angle grain boundaries may evolve during high temperature deformation in ways other than the nucleation and growth of grains at pre-existing boundaries, and in this section we examine some of these alternative mechanisms of dynamic recrystallization. Although such processes generally fall into the overall phenomenological classification of **continuous dynamic recrystallization,** it must be recognised that within this category there are several quite different types of mechanism which need to be considered separately.

There are at least two processes which can be classed as continuous dynamic recrystallization. The first, known as **geometric dynamic recrystallization,** has many similarities with the continuous recrystallization which occurs on annealing alloys which have undergone very large strains, and for this reason it is discussed in detail in chapter 14. The other process, found in both metals and minerals, and which involves a gradual rotation of the material adjacent to high angle boundaries, is discussed below.

13.4.2 Dynamic recrystallization by progressive lattice rotation

There is considerable evidence that in certain materials, new grains with high angle boundaries may be formed during straining, by the progressive rotation of subgrains with little accompanying boundary migration. This is a **strain-induced** phenomenon which should not be confused with the subgrain rotation which has been postulated to occur during static annealing (§6.5.4).

The phenomenon involves the progressive rotation of subgrains adjacent to pre-existing grain boundaries as the material is strained, with the old grains developing a gradient of misorientation from centre to edge. In the centre of the old grain, subgrains may not be well developed or may have very low misorientations. Towards the grain boundary, the misorientations increase, and at larger strains, high angle boundaries may develop. This type of mechanism was first found in minerals (see §13.5), and has since been found in a variety of non-metallic and metallic materials. In the Geological literature the phenomenon is termed **rotation recrystallization.**

The mechanisms by which this progressive subgrain rotation occurs are not yet entirely clear, but it is most frequently found in materials in which dislocation motion is inhibited by either a **lack of slip systems** (e.g. magnesium alloys) or by **solute drag** (e.g. aluminium–magnesium alloys). It is likely that it is associated with inhomogeneous plasticity and accelerated dynamic recovery in the grain boundary regions, and it is possible that grain boundary sliding is also involved. However, the occurrence of a transition in dynamic recrystallization behaviour in minerals between discontinuous and rotation mechanisms (§13.5), raises the possibility that dynamic recrystallization by subgrain rotation in cubic metals may occur when boundaries are solute-loaded and unable to migrate rapidly (§5.4.2). Although this phenomenon usually results in a partially recrystallized **necklace** microstructure (fig. 13.14a–c), at large strains a completely recrystallized structure (fig. 13.14d) may be formed (Gardner and Grimes 1979).

13.4.2.1 Magnesium alloys

There is evidence that progressive lattice rotation may occur at grain boundaries in magnesium alloys (Ion et al. 1982, Galiyev et al. 2001, Tan and Tan 2003), and that this may eventually lead to the formation of new grains. The mechanism proposed by Ion et al. (1982), which is shown schematically in figure 13.20, is based on local shearing near grain boundaries (fig. 13.20a), which occurs because of the lack of the 5 independent slip systems required for homogeneous plasticity (§3.7). Dynamic recovery of the geometrically necessary dislocations then occurs (fig. 13.20b), resulting in the formation of new subgrains or grains (fig. 13.20c). Such a process is progressive, with no clear division between the nucleation and growth stages. At higher deformation temperatures, non-basal slip is easier, deformation becomes more homogeneous, and the dynamic recrystallization becomes similar to the discontinuous process discussed in §13.3 (Galiyev et al. 2001).

13.4.2.2 Aluminium alloys

In aluminium alloys containing solute additions such as Al–Mg alloys (Gardner and Grimes 1979, Drury and Humphreys 1986) and Al–Zn alloys (Gardner and Grimes

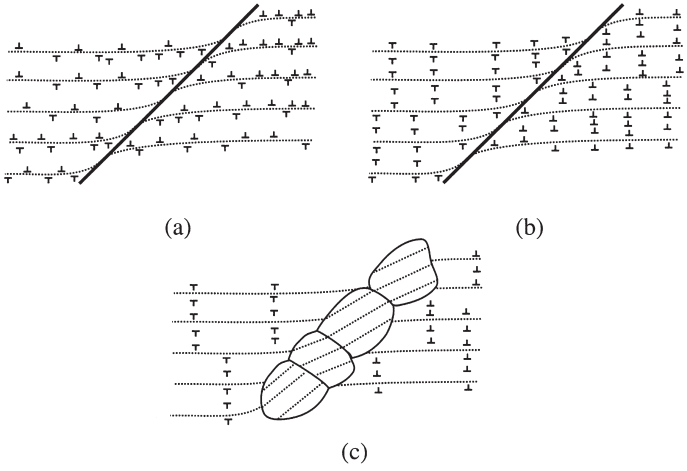

Fig. 13.20. Schematic diagram showing the proposed mechanism of dynamic recrystallization in magnesium, by progressive lattice rotation and dynamic recovery at grain boundaries, (after Ion et al. 1982).

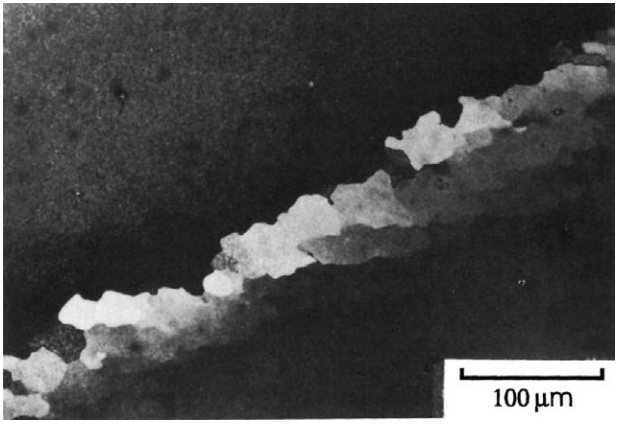

Fig. 13.21. Development of misorientations by lattice rotation adjacent to the grain boundary during deformation of Al–5%Mg, (Drury and Humphreys 1986).

1979), significant lattice rotations may develop at the grain boundaries during deformation at temperatures in the range 300–400°C. Even though there is little evidence of subgrain formation in the grain interiors, well developed subgrain/grains may develop at the boundaries as seen in figure 13.21.

Investigation of these microstructures by EBSD has enabled the development of such microstructures to be determined in some detail. Figure 13.22 shows an EBSD map of a grain boundary region in Al–5%Mg deformed in plane strain compression at 350°C. The original high angle boundary is denoted by a thick line and the low angle

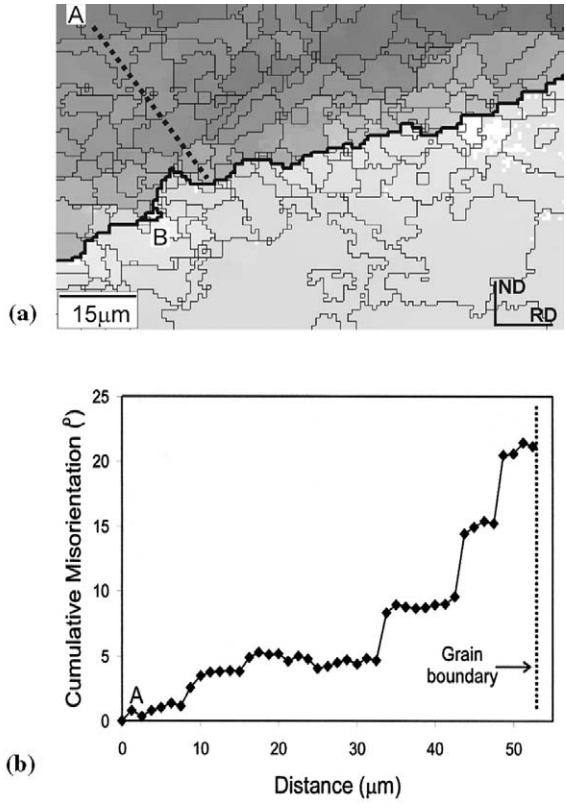

Fig. 13.22. EBSD measurements of lattice rotations at a grain boundary in Al–5%Mg, deformed in plane strain compression at 350°C. (a) EBSD map showing high angle (> 15°) boundaries as thick lines and low angle boundaries as thin lines. Colour changes reveal misorientations developed at the boundary serrations, (b) The cumulative misorientations along the line from A to the boundary. (See colour plate section for fig. 13.22a.)

boundaries by thin lines. A plot of the cumulative misorientation from the interior of the grain (A) to the boundary, along the dotted line (fig. 13.22b), shows the large orientation gradients which develop at the boundaries, particularly within the serrations. In figure 13.22, these have not yet developed into separate identifiable grains, except at B.

It has been proposed that the mechanism involves an interaction between grain boundary deformation and the grain boundary serrations (Drury and Humphreys 1986) as shown in figure 13.23. High angle grain boundaries develop serrations due to interaction with the deformation substructure (fig. 13.5a), as shown in figure 13.23a. Grain boundary sliding can then only occur on parts of the boundary, e.g. A, whilst other regions (e.g. B) have to accommodate the strain by plastic deformation (fig. 13.23b), leading to shear and local lattice rotation as shown in figure 13.23c. Whether

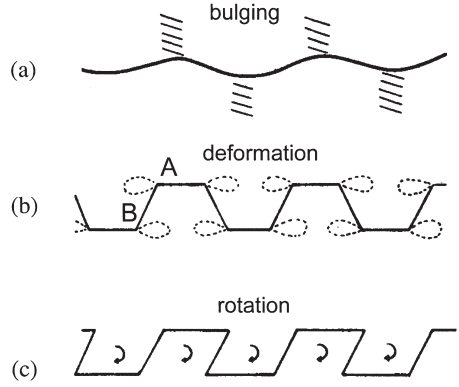

Fig. 13.23. Proposed mechanism of dynamic recrystallization by progressive lattice rotation in Al–Mg alloys. (a) HAGB serrations form, (b) Grain boundary sliding occurs on horizontal boundaries, but slip occurs on bulged sections, leading to local lattice rotations associated with the bulges, (c), (Drury and Humphreys 1986).

the deformation at the boundaries involves actual grain boundary sliding, or local plasticity close to the boundaries is not yet established.

It is interesting to note that it has recently been suggested that the mechanism of figure 13.23 may be responsible for the nucleation of discontinuous dynamic recrystallization in copper (Wusatowska et al, 2002).

13.4.2.3 Particle-stabilised microstructures

It has been suggested that a process similar to that of progressive lattice rotation discussed above, may occur in alloys containing finely dispersed second-phase particles, and that this mechanism may be responsible for the development of fine grained microstructures during the thermomechanical processing of superplastic aluminium alloys (§15.5.3). It was proposed that the particles pinned the subgrains, preventing extensive growth, and evidence of a progressive increase of the subgrain/grain misorientation has been claimed (Nes 1979, Higashi et al. 1990). However, this behaviour is generally observed in alloys which have already been extensively cold or warm worked, and more recent work carried out with the benefit of EBSD (Ridley et al. 2000), suggests that the development of subgrain misorientations during hot deformation of fine-grained aluminium alloys containing dispersions of small stable Al_3Zr particles, does not differ significantly from that in single-phase alloys (§13.2), and that any increase in the fraction of high angle boundaries is primarily due to a decrease in the number of low angle boundaries. The development of superplastic microstructures by hot working is further discussed in §15.5.3.

13.5 DYNAMIC RECRYSTALLIZATION IN MINERALS

Dynamic (or **syntectonic**) recrystallization has long been recognised as an important process during the natural deformation under metamorphic conditions, of rock-forming

minerals (see e.g. Nicolas and Poirier 1976, Poirier and Guillopé 1979, Poirier 1985, Urai et al. 1986, Urai and Jessel 2001). Although there are substantial differences not only between minerals and metals, but also between the deformation conditions in the Earth's crust and mantle, and in a hot-rolling mill, there is a substantial commonality of behaviour between the two classes of materials, and over the past 30 years there has been a very fruitful interchange of scientific ideas between Geology and Materials Science. One of the main interests of the Geologists is in using the microstructure to interpret the deformation history of the mineral. The dynamically recrystallized grain sizes (fig. 13.17), which have been shown to be closely related to stress (equation 13.18) have, together with the subgrain sizes and dislocation densities, been used by Geologists as **paleopiezometers** to determine the stresses to which the mineral has been subjected.

Research in this area has involved the investigation of microstructures in naturally deformed minerals, laboratory deformation of minerals under conditions of high temperature and high pressure, and the in-situ deformation under the optical microscope of low melting point minerals and other transparent analogue crystalline materials. The latter experiments (e.g. Means 1989) have been able to provide direct observations of the occurrence of dynamic recrystallization, albeit at low spatial resolution, that cannot be obtained for metals. In many cases it is also possible to simultaneously obtain local orientation (microtexture) information from minerals in the optical microscope using standard mineralogical methods. Figure 13.24 is an optical micrograph of a naturally deformed quartzite and shows clear evidence of dynamic recrystallization in the regions of the original grain boundaries. Figure 13.25 is an example of an in-situ deformation experiment on camphor, showing the development of a similar microstructure to figures 13.15 and 13.24.

13.5.1 Boundary migration in minerals

Natural minerals are generally very impure, and segregation and precipitation may occur at the grain boundaries leading to a loss of mobility. In addition, bubbles and

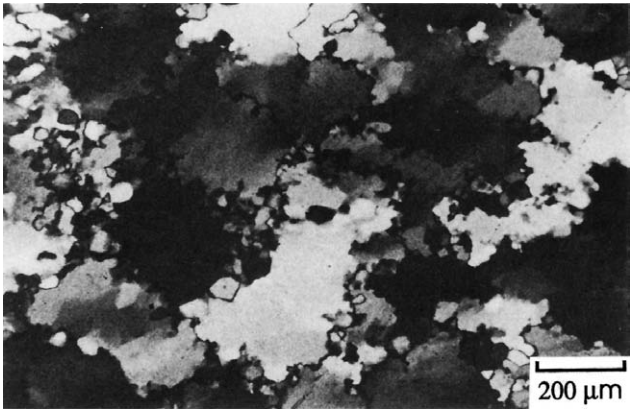

Fig. 13.24. Dynamic recrystallization in naturally deformed quartzite, (Urai et al. 1986).

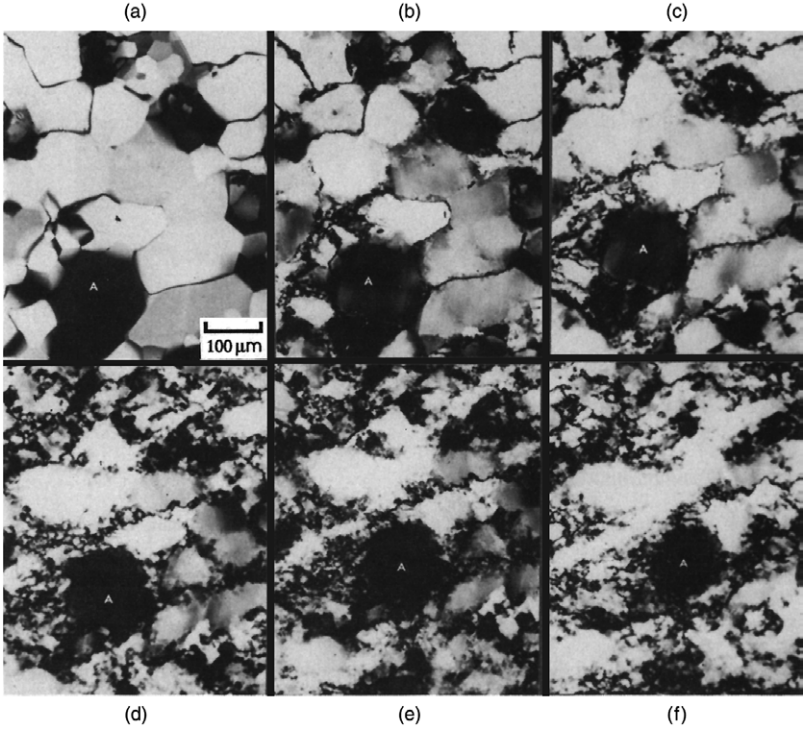

Fig. 13.25. Dynamic recrystallization of camphor at room temperature, (Tungatt and Humphreys 1981).

cavities may also be present. The bonding in minerals is of course different to that in metals, and this will also influence the boundary migration (Kingery 1974, Brook 1976). In many instances, the boundaries in minerals are likely to resemble those of impure ceramics.

It is now well established that in some natural minerals there is a fluid film at the boundary (see Urai et al. 1986, Urai and Jessel 2001) and that this has a large influence on grain boundary migration (Rutter 1983). The structure of a fluid-filled boundary can be described in terms of the two crystal–liquid interfaces and the fluid layer between them, and the behaviour of the boundary will therefore be less constrained by the matching of the two crystals than for a dry boundary. The boundary configuration may then be determined by the energy of the crystal–liquid interfaces, as is the case for crystal growth from the melt, and an orientation dependence of boundary migration rate is therefore expected. Migration mechanisms related to solid–liquid interfaces such as spiral growth involving screw dislocations (cf. Gleiter's boundary migration model discussed in §5.4.1.3) are predicted to be important.

If it is assumed that the migration rate is limited by diffusion in the fluid layer, a rapid increase in migration rate with film thickness is predicted as shown qualitatively in

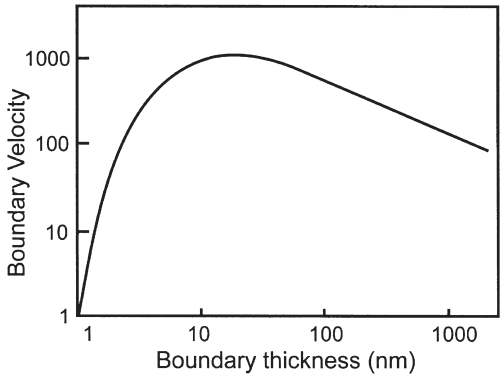

Fig. 13.26. The predicted effect of fluid film thickness on boundary migration rate, (Urai et al. 1986).

figure 13.26. The increase in mobility may be as much as four orders of magnitude for a 2nm film (Rutter 1983). For thick fluid layers, diffusion across the film is expected to become rate controlling, the mobility then becoming inversely proportional to the film thickness.

13.5.2 Migration and rotation recrystallization

It is well established that in minerals, two types of dynamic recrystallization occur. At high temperatures and high stresses a discontinuous form of dynamic recrystallization similar to that discussed in §13.3 occurs, and this is referred to in the Geological literature as **migration recrystallization**. However, at lower temperatures and stresses there is often a transition to a mechanism similar to that discussed in §13.4 (referred to as **rotation recrystallization**). This transition, which is thought to correspond to the breakaway of boundaries from their solute atmospheres (fig. 5.32), is shown in figure 13.27 for experimentally deformed halite (NaCl). The driving force for dynamic recrystallization increases with applied stress and the intrinsic boundary mobility is also a strong function of temperature, thus accounting qualitatively for the shape of figure 13.27. It has also been shown (Trimby et al. 2000) that the transition between rotation and migration recrystallization in NaCl is dependent on the water content of the material. The boundary mobility in ionic solids is very sensitive to small solute concentrations, particularly aliovalent ions, and in figure 13.28, it is seen that the transition temperature in $NaNO_3$ (calcite structure) between rotation and migration recrystallization is markedly raised by small amounts of Ca^{2+} ions.

13.6 ANNEALING AFTER HOT DEFORMATION

Recovery and recrystallization following hot deformation are of great technological importance because in many hot working operations such as multi-pass rolling,

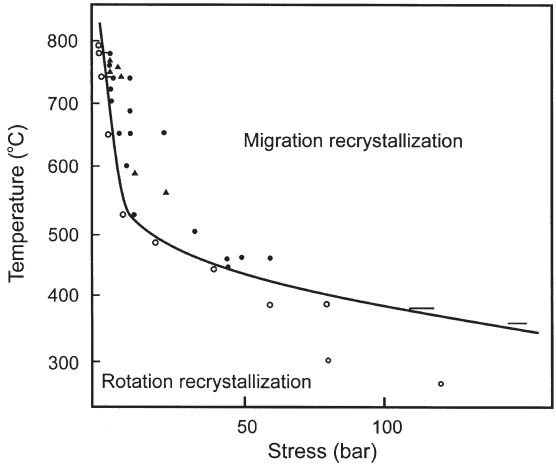

Fig. 13.27. The boundary between migration and rotation recrystallization in halite, (Guillopé and Poirier 1979).

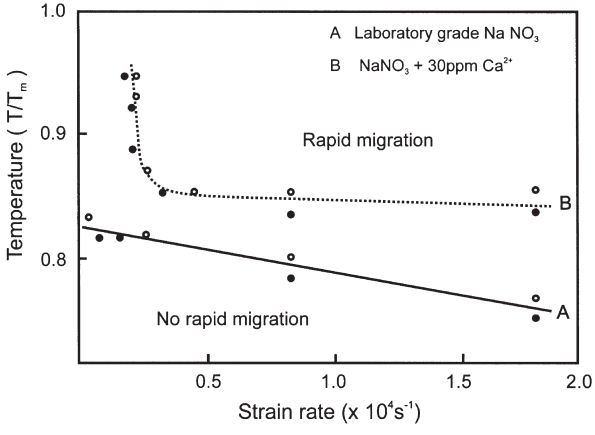

Fig. 13.28. The effect of calcium additions on boundary migration in sodium nitrate, (Tungatt and Humphreys 1984).

annealing takes place between the rolling passes. Additionally, the rates of cooling of the material are generally very low in large-scale metal forming operations, allowing recovery, recrystallization and grain growth to occur immediately after hot deformation.

13.6.1 Static recovery

Because dynamic recovery has already taken place during the deformation, further microstructural changes due to static recovery are generally small. However, some

further recovery, including dislocation rearrangement and subgrain growth (Ouchi and Okita 1983) and consequent softening (Sellars et al. 1986) may take place, usually with similar kinetics to those found for static recovery (§6.2.2).

13.6.2 Static recrystallization

Static recrystallization may occur when a hot deformed material is subsequently annealed. This is often very similar to the static recrystallization discussed in earlier chapters, the main difference being that the lower stored energy resulting from hot deformation, affects the kinetics of recrystallization. From §13.2.1 we expect the driving pressure and hence the recrystallization behaviour to be strongly dependent on **Z,** and this effect is well documented (see Jonas et al. 1969). Figure 13.29 shows the effect of **Z** on the recrystallization kinetics of commercially pure aluminium deformed to a constant strain and annealed at a constant temperature. The effect of strain is also important, and in materials which undergo dynamic recrystallization, the static recrystallization behaviour depends on whether the strain was larger or smaller than that required for dynamic recrystallization (ε_c).

Because of the industrial importance of controlling the grain size and texture during the recrystallization of hot-rolled aluminium alloys, there has been significant activity in investigating the mechanisms of recrystallization in these materials. Much attention has focussed on the nucleation of cube-oriented grains, and it is now thought that these originate from elongated remnants of cube grains in the hot-worked microstructure (Vatne et al. 1996a), by a process of strain induced boundary migration such as described in §7.6.2. A more detailed consideration of the formation of cube grains during recrystallization of hot deformed aluminium can be found in §12.4.1.

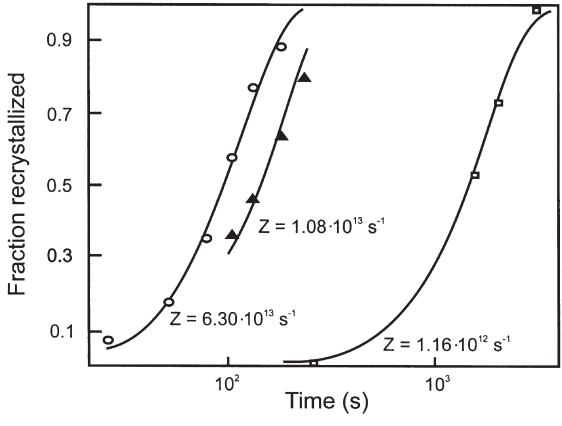

Fig. 13.29. The effect of deformation temperature and strain rate (Zener–Hollomon parameter) on the recrystallization kinetics of commercial purity aluminium deformed to a strain of 3 and annealed at 410°C, (Gutierrez et al. 1988).

Metallographic measurements indicate that static recrystallization can often be described approximately by the JMAK relationship (equation 7.17), with the exponent in the range 1.5–2 (Roberts 1984, 1985). Because of the technological importance of the subject, empirical relationships for the recrystallization behaviour as a function of deformation behaviour have been determined (e.g. Roberts 1985, Sellars 1986, 1992a, Beynon and Sellars 1992), and for C–Mn and HSLA steels of grain size $\mathbf{D_0}$, it is often found that the time for 50% static recrystallization ($t_{0.5}$) at the deformation temperature is given (Sellars and Whiteman 1979) by an equation of the form

$$t_{0.5} = c_1 D_0^C \varepsilon^{-n} Z^{-K} \exp\left(\frac{Q_{rex}}{RT}\right) \tag{13.21}$$

where c_1, C, K and n are constants and Q_{rex} is the activation energy for recrystallization.

The recrystallized grains generally nucleate at the old grain boundaries and are equiaxed. Their size $\mathbf{D_R}$ is given by

$$D_R = c_2 D_0^{C'} \varepsilon^{-n'} Z^{-K'} \tag{13.22}$$

where c_2, C′, K′ and n′ are constants.

The range of values of the constants in these equations is discussed by Roberts (1985) and Sellars (1986, 1992a). If dynamic recrystallization has occurred prior to static recrystallization, then there is little effect of strain or D_0, i.e. C, C′, n and n′ tend to zero. Relationships such as these are necessary components of models for industrial hot rolling (§16.3) and much recent research effort has been aimed at developing physically-based state-variable constitutive annealing models to describe recrystallization following hot deformation (e.g. Sellars 1997, Furu et al. 1996, Vatne et al. 1996b). The annealing of the hot worked materials are modelled by the incorporation of processes such as dislocation recovery, SIBM and PSN into deformation microstructures modelled using the principles discussed in §13.2.5.

13.6.3 Metadynamic recrystallization

Whenever the critical strain for dynamic recrystallization (ε_c) is exceeded, recrystallization nuclei will be present in the material. If straining is stopped, but annealing continued, these nuclei will grow with no incubation period into the heterogeneous, partly dynamically recrystallized matrix. This phenomenon is known as **metadynamic recrystallization** (Djaic and Jonas 1972, Petkovic et al. 1979). The microstructure of a material which has undergone some dynamic recrystallization is very heterogeneous and may contain:

A – Small dynamically recrystallized grains (nuclei) which are almost dislocation free.
B – Larger recrystallized grains with a moderate dislocation density which are growing dynamically.
C – Unrecrystallized material with a high dislocation density (ρ_m).

Each of these types of region will have a different static annealing behaviour, and the overall annealing kinetics and grain size distributions may be extremely complex, as

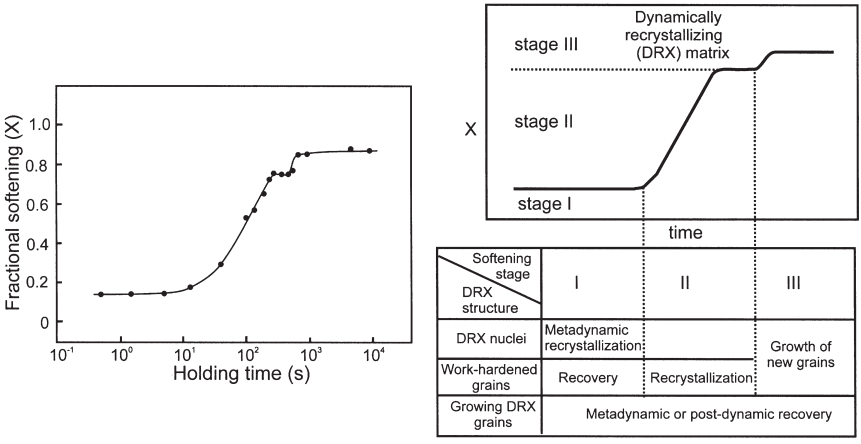

(a) (b)

Fig. 13.30. The restoration processes occurring in a dynamically recrystallizing material if it is held at temperature after deformation has stopped. (a) The effect of strain on the static softening of austenite deformed at 860°C, (Xu and Sakai 1991), (b) Schematic relationship between the various softening stages and the main restoration processes, (Xu et al. 1995).

illustrated by figure 13.30a. Sakai and colleagues (Sakai et al. 1988, Sakai and Ohashi 1992, Sakai 1997) have identified several annealing stages in hot-deformed nickel, copper and steels.

- **Regions A,** may continue to grow during the early stages of post deformation annealing by the mechanism of metadynamic recrystallization.

- **Regions B** will, if their dislocation density (ρ) is below a critical value (ρ_{RX}), recover, and this has been termed **metadynamic recovery.** If $\rho > \rho_{RX}$ then these regions may subsequently recrystallize statically.

- **Regions C** will undergo static recovery, followed by static recrystallization. When the material is fully recrystallized then further grain growth may occur (§13.6.5). The relationship between the various restoration processes and the overall softening is shown schematically in figure 13.30b.

13.6.4 PSN after hot deformation

The conditions under which particle stimulated nucleation of recrystallization (PSN) could occur following low temperature deformation were discussed in §9.3. However, if the temperature of deformation is raised, then PSN may become less viable, and we need to consider the effect of deformation temperature on the two criteria for PSN – the **formation** of nuclei within deformation zones, and the **growth** of the nuclei beyond the particle.

13.6.4.1 Deformation zone formation

At high temperatures, dislocations may be able to bypass particles without forming deformation zones. Humphreys and Kalu (1987) have shown that the critical strain rate for the formation of a deformation zone at a particle of diameter **d** is given by:-

$$\dot{\varepsilon}_c = \frac{K_1 \exp\left(\frac{-Q_s}{RT}\right)}{Td^2} + \frac{K_2 \exp\left(\frac{-Q_b}{RT}\right)}{Td^3} \tag{13.23}$$

where K_1 and K_2 are constants and Q_s and Q_b are the activation energies for volume and boundary diffusion. This relationship has been found to be obeyed in aluminium alloys for a wide range of particle sizes and deformation conditions with $K_1 = 1712 m^2 s^{-1} K$ and $K_2 = 3x10^{-10} m^3 s^{-1} K$.

For particles which are potential PSN sites ($d > 1\mu m$), the second term will generally be negligible, and a simplified version of equation 13.23 may therefore be used. The critical particle diameter for the formation of a particle deformation zone (d_f) may, if we assume that the activation energies in equations 13.1 and 13.23 are identical, be expressed in terms of the Zener–Hollomon parameter as

$$d_f = \left(\frac{K_1}{TZ}\right)^{1/2} \tag{13.24}$$

13.6.4.2 Nucleus growth

The growth criterion for PSN (e.g. equation 9.24) is also affected by the deformation conditions, because the stored energy (E_D) is reduced at elevated temperatures, although this effect is more difficult to quantify. As the microstructure following high temperature deformation consists mainly of subgrains, the growth condition (equation 9.2) may be written in terms of the subgrain size (D), using equation 2.7, as

$$d_g = \frac{4\gamma_b D}{3\gamma_s} \tag{13.25}$$

and using equation 13.7 then

$$d_g = \frac{4\gamma_b K G b}{3\gamma_s \sigma} \tag{13.26}$$

The relationship between the flow stress (σ) and Zener–Hollomon parameter is given by equations 13.2 to 13.5, and if, for example we use equations 13.1 and 13.4 then

$$d_g = \frac{4\gamma_b K' G b}{3\gamma_s Z^{1/m}} \tag{13.27}$$

Somewhat different versions of equation 13.27 may be obtained, depending on the particular relationships between subgrain size, flow stress and **Z** which are used, and at present there is no entirely satisfactory solution.

In figure 13.31 we show the variation of the critical particle diameters for the formation and growth of particle deformation zones, with **Z,** according to equations 13.24 and 13.27 (neglecting the small effect of the temperature term in equation 13.24 and using values of the constants appropriate for aluminium). It may be seen that at values of **Z**

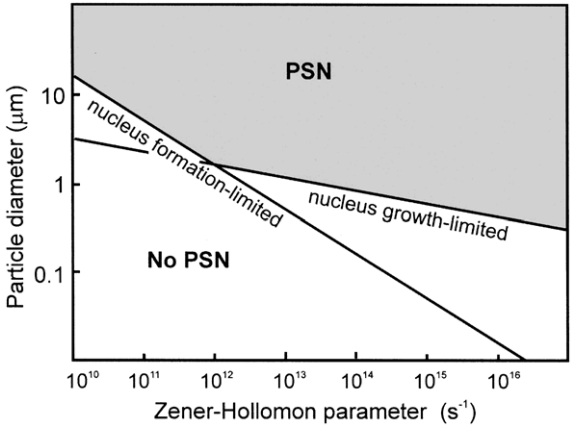

Fig. 13.31. The effect of deformation conditions on PSN.

less than $\sim 10^{12}$ s^{-1}, the condition for PSN is governed by that for **deformation zone formation,** but at higher values it is determined by the criterion for **growth** of the nucleus. Experimental investigations have confirmed this model. Measurements by Kalu and Humphreys (1986) on Al–Si alloys deformed at $10^8 < Z < 10^{12}$ showed that zone formation was the controlling factor, whereas the measurements of Oscarsson et al. (1987) on AA3004 and of Furu et al. (1992) on AA3003, in which specimens were deformed in the range $10^{12} < Z < 10^{16}$, were both consistent with growth control.

13.6.5 Grain growth after hot working

When recrystallization is complete, grain growth can take place, and has been described by the empirical equation

$$D^n = D_R^n + c\,t\exp\left(-\frac{Q_g}{kT}\right) \tag{13.28}$$

where c, n and Q_g are constants.

For steels, very large values of the exponent n ($\sim$10) have been reported (see Sellars 1986).

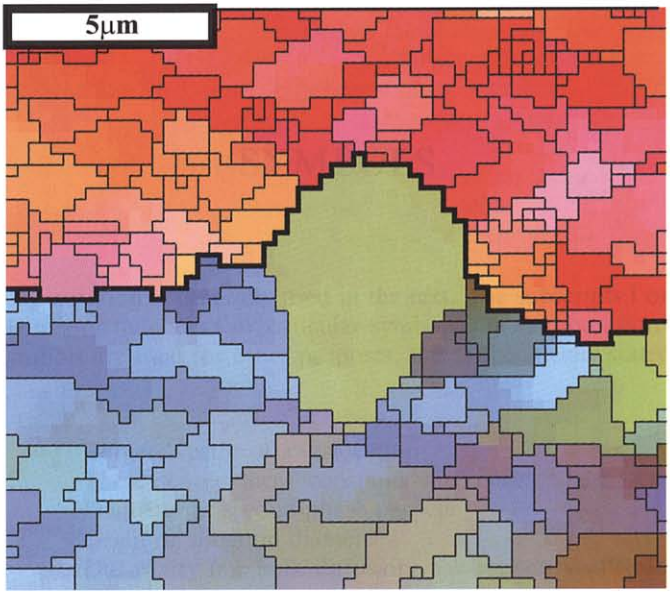

Fig. 7.31. See p. 257.

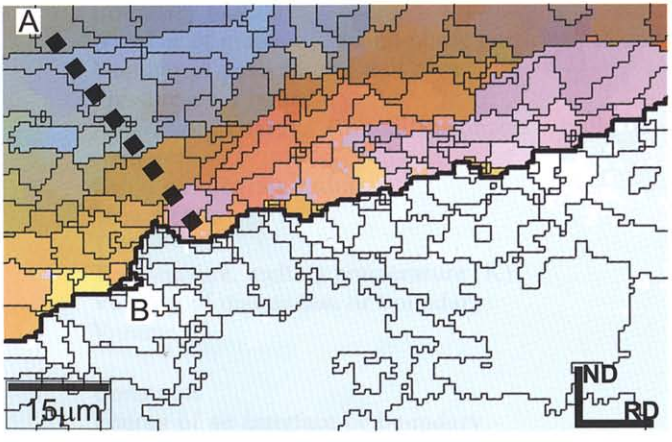

Fig. 13.22(a). See p. 440.